APPLICATION OF FRACTURE MECHANICS TO THE PREDICTION OF RUPTURE BEHAVIOUR OF THIN CYLINDRICAL STRUCTURES

B. HENRY

Technology Division, J.R.C. EURATOM, I-21020 Ispra (Varese), Italy;
Commission of the European Communities

SUMMARY

The paper deals with the prediction of rupture in thin tubing as those of primary piping of LMFBR.

Burst tests on part-through cracked tubes in type AISI 304 having an external diameter of 178 mm and a thickness of 6,5 mm have been undertaken at room temperature and 380°C with the following scopes:

a) to check the validity of available formulae (R.J. Eiber, J. Dufresne) allowing to predict the rupture of the ligament;
b) to check the validity of previous work by the author inspired by Hahn and Rosenfeld work allowing to predict whether the corresponding through crack, consecutive to the ligament rupture, will be stable or unstable.

As far as the first point is concerned, the results show that the formulae give a reasonable description of the ligament rupture, under the condition that a valid value of the parameter describing the fracture resistance on the flow properties be introduced in the formulae. However, this valid value does not seem accessible to a specimen test and therefore these approaches seem unsufficient for an absolute prediction, given a combination of material and geometry, and using specimen data.

As far as the second point is concerned, the experiments evidence that the frontier between unstable catastrophic rupture (under gas pressurization) and leakage for a given crack length is always at a stress higher than that corresponding to the unstability (maximum pressure) of the through crack of the same length in hydraulic tests, using a sealing patch. Exagerate correction of the patch effect in the latter tests and shortage of energy in the present tests under gas may both contribute to this discrepancy. The prediction based on the through crack tests data appears in any case as a lower bound an is recommended.

The possibility to predict the critical crack length for unstability on the basis of specimen tests data—tensile and C.O.D.—is also dealt with in the paper, on the basis of previous C.O.D. tests on C.T. specimens. It is concluded that while an "absolute" prediction seems unreliable, a "relative" prediction seems suitable, using the specimen data in a correction factor. This allows to transfer tube test results from the reference conditions of the material (for instance: room temperature, undamaged) to the conditions of interest (for instance: high temperature, embrittled).

1. Introduction

Both LMFBR and LWR involve a large use of thin or relatively thin austenitic stainless steel tubing for the piping system. For such applications, linear elastic fracture mechanics is not usable due to the high material toughness and the low (or relatively low) thickness. However the evaluation of the significance of defects in the tubing material, specially in connection with a possible toughness degradation due to environmental effects [1], is very important for the fracture control plan of the primary containment.
In a previous work [2], [3] the problem of crack instability in type AISI 304 austenitic stainless steel tubing was approached, on the basis of the results of through cracked tube tests. Using a stress intensity factor formulation proposed by Hahn et al. [4], a value of the fracture toughness K_c could be obtained from tests, which was not too much dependent neither of the tubing geometry - within the investigated dimensions range - nor of the crack length under the condition that an idoneous correction factor for curvature M, which had to take in account the interaction of the patch used to seal the through cracks be used in the K_c formulation. It was felt useful to investigate how far this K_c value allows to predict the behaviour - namely leakage or failure - of more realistic part through cracked tubes at the rupture of the remaining ligament. One could expect that when the depth of the part through crack is sufficient to produce the ligament rupture at a gross stress level inferior to the critical stress of a through crack of the same length, leakage would follow while crack propagation would result of ligament rupture at a stress level superior to the through crack critical stress. A systematic variation of the crack depth at a fixed length should therefore permit to find the instability stress and to compare it with the results of the through cracked tube tests.
Moreover it was intended to compare various theories of the part-through crack failure specially developped for thin cracks and plasticized ligaments when applied to this practical situation of thin austenitic stainless steel tubing.
This latter aspect is dealed with in section 3 of this paper, while the problem of crack instability is discussed in section 4.

2. Experimental Details and Results

The tests have been achieved at room temperature and 540° C on tube sections in type AISI 304, external diameter 176 mm, thickness 5 to 6 mm, length 400 to 500 mm: Composition and reference tensile properties of this material are given in table I.
The tube sections were machined on a lathe in order to obtain a well defined and constant thickness, at least in the region of the slot.
In each tube section, a longitudinal part-through slot was machined by electro-erosion according to a rectangular profile. Their width was smaller than 0,5 mm. Their length was either 75 mm or 150 mm, and their depth was varied between 60% and 90% of the wall thickness.
The tube sections were closed by two flat heads welded at both ends. For the tests at 540 ° C an heating system consisting of Ni-Cr wire wound on a ceramic support was centered and shut up inside the tube section. The heating system was lost each time the tube failed catastrophically. The tube was insulated by glass wool and asbestos bands.
It was checked previously that when the temperature was maintained at 540° C on the center of the crack, it was 25 °C down at 150 mm from the crack center on the same generatrice and 8 °C down on a point diametrally opposed to the crack center.
The tubes were connected to a nitrogen container and pressurized by a manual progressive action on the pressure regulator of the container. The pressure was measured at the entrance of the tube by a pressure transducer and plotted us. time on a Leeds & Northrup potentiometric plotter. Pressurization rates ranged between 50 and 150 atm/min according to the test.
The results are reported on tables II and III and on the figures : gross hoop stress at failure vs. the ratio crack depth/wall thickness, p/e, fig. 1 and 2, and gross hoop stress at failure vs. the shell parameter $\lambda = \frac{a}{\sqrt{Re}} (1-\nu^2)^{1/4}$ (fig. 3 and 4). On these latter and

in tables II and III, the propagation behaviour is visualized according the following classification :

- castastrophic failure (P) : the tube section was completely destroyed, by a full length propagation, involving also the heads.
- propagation and arrest (P+A) : the crack propagated and arrested before the head welds. The propagation length is reported on tables I and II.
- initiation (I) : some crack extension was visible at the slot ends but not measurable.
- leakage (L) : the ligament broke without any extension of the rupture to the tube wall.

The general trend of these results is satisfactory as far as the monotonic variation of σ_h^c vs. p/e is concerned, and also when considering the progressive change from leakage to catastrophic failure when σ_h^c increases (or $\frac{p}{e}$ decreases). The only exception is test nr. 5 at 540°C for which the burst hoop stress is surprisingly high (fig. 2).

3. Analysis and discussion of the part-through crack failure data.

Three different modelling of the part-through crack failure have been considered to analyse the above results.

The first one is that of Eiber and al.[5]. It is based on a flow stress concept, and combines in an empirical way the effect of the reduction of the wall thickness (ratio p/e) and that of the curvature (correction factor M depending on the shell parameter $\frac{a}{\sqrt{Rt}}$).

The gross hoop stress for failure of the ligament is given by :

$$\sigma_h = \bar{\sigma} \cdot \frac{1 - \frac{p}{e}}{1 - \frac{p}{e} \cdot \frac{1}{M}} \qquad \text{eq. (1)}$$

The second one is that of Carlsson [6] . It assumes an elastic-ideal plastic behaviour (yield strenght σ_y) and represents the crack by a zone of reduced yield strenght σ_{yi} where $\sigma_{yi} = (1 - \frac{p}{e}) \frac{2}{\sqrt{3}} \sigma_y$. The displacement at the center of the crack is then given by :

$$\delta = \frac{4 \sigma_y a}{E} D (S_\infty, Si) \qquad \text{eq. (2)}$$

where D is a numerical function of $S_\infty = \frac{\sigma_h}{\sigma_y}$ and $Si = \frac{\sigma_{yi}}{\sigma_y} = (1 - \frac{p}{e}) \frac{2}{\sqrt{3}}$.

The expression of D given by Carlsson in [6] may be reduced to the simpler form :

$$D = \frac{S_\infty - S_i}{1 - S_i} + (1 - Si) \frac{2}{\pi} \operatorname{Log} \frac{\cos \beta + 1}{\sin \beta} \quad \text{where } \beta = \frac{\pi}{2} \frac{1 - S_\infty}{1 - S_i}$$

Assuming that the ligament fails for a critical value of the displacement $\delta = \delta_c$, the relationship (2) allows to calculate the hoop stress at failure vs. the crack geometry and the material properties. For strain-hardening materials, Carlsson suggests to substitute in the above formula σ_y by a flow stress $\bar{\sigma}$ ($\sigma_y < \bar{\sigma} < \sigma_u$), to be determined empirically.

The third model we have considered has been recently proposed by Dufresne [7] . The physical approach is quite near of the Carlsson' one, but the mathematical treatment is different. The flow properties are introduced by the monoaxial tensile properties σ_y and σ_u : thus no arbitrary flow stress has to be chosen. Like in the Carlsson' model, no consideration is brought to curvature effects. The Dufresne'expressions useful in practice are :

$$\frac{\sigma_h}{\sigma_y} = \frac{(1 - \frac{p}{e})(\frac{\sigma_u}{\sigma_y} + 1) \frac{\cos \alpha}{2} + \frac{2\alpha}{\pi} \frac{p}{e}}{\frac{p}{e} + (1 - \frac{p}{e}) \cos \alpha} \qquad \text{eq. (3)}$$

$$\text{with : } \alpha = 2 \operatorname{Arctg} \left\{ \exp \frac{\pi e}{p} \left[\frac{\delta E}{8 a \sigma_y} + \frac{1}{6} \left(\frac{\sigma_u}{\sigma_y} - 1 \right) \left(1 - \frac{p}{e} \right) \right] \right\} - \frac{\pi}{2} \qquad \text{eq. (3')}$$

where δ has the same physical significance as in the Carlsson' model (crack opening displacement at the crack center).
For the application of the three models the value of the flow or critical parameters have first been calculated using the test data : formula (1) produced $\bar{\sigma}$ values, while formula (2) and (3) - (3') produced δ values. For the application of (2), a flow stress value equal to $\frac{\sigma_y + \sigma_u}{2}$ has been arbitrarily chosen. The resulting values for $\bar{\sigma}$ (Eiber'model) and δ (Carlsson' and Dufresne'models) appear on tables II and III.
A first evaluation of the three models may be attempted on the basis of these values.
Even if it demonstrates some trend to increase when p /e increases, $\bar{\sigma}$ (Eiber'model) appears fairly constant for all the tests series at the same temperature (standard deviation $\pm$ 12 %). However while it is greater than σ_u in the room temperature test (61 against 53 kg/mm^2), it is about equal to $\frac{\sigma_y + \sigma_u}{2}$ in the 540°C tests (29,6 against 25,5 kg/mm^2).

The C.O.D. of the Carlsson'model, δ_C, demonstrates satisfactory trends : its scatter is reduced (standard deviation $\pm$ 17-20%) with no systematic variation vs. p/e variation. Its decrease with temperature was expected as well but its absolute value is about 4 times lower than that measured on 8 mm thick C.T. specimen of the same material [1].
It is evident that constraint conditions are not at all similar in the two situations and a correct measurement of δ to be applied in this model would require a deeply cracked specimen with a large width in respect to its thickness.

The C.O.D. of the Dufresne'models δ_D is significantly scattered (standard deviation : $\pm$ 45 % to 83%), with a trend to decrease when p/e is increased in the room temperature tests. The mean value is significantly lower than δ_C. Note that δ_D cannot be computed for all the tests where $\sigma_h > \sigma_y$: as a matter of fact, the models takes in account the strain hardening in the ligament but assumes that the gross stress remains below the yielding limit.

The mean values of $\bar{\sigma}$, δ_C and δ_D have been used to calculate theoretical curves of σ_h at failure vs. p/e, using (1) or (2) or (3) -(3'); they are reported in fig. 1 - 2.
The fact that these curves converge in the tested range of p /e is nothing but a consequence of the fitting procedure. These curves vizualize the significantly different behaviour of the three models in describing the influence of the crack depth, p /e. A larger experimental variation of this parameter would be necessary to better differentiate the models from this point of view. As a general trend, however it appears that the Carlsson'model fits better to the experimental results. This feature is confirmed by fig. 6-7 where the calculated values of σ_h at failure are plotted vs. the experimental ones. Only the points relative to the Carlsson'model are all within a scattering band of $\pm$ 10 % for the both series of tests.
The capacity of the models to be used for the prediction of the structure behaviour requires furthermore that the material parameters entering it be accessible by tests on specimen or at least on sub-scale identically shaped structures.
As far as the Eiber'model is concerned, the lack of an identical relationship, for both room temperature and 540°C testing, between $\bar{\sigma}$ and the tensile properties is unhappy from this point of view. In order to check if at least at a given temperature i.e. for a given strain hardening behaviour the flow stress presents some fixed correlation with the tensile properties - indepently from the geometry, tests at 540°C on AISI 304 tubing 89 mm O.D. and 3,5 mm thick reported by Dufresne [7] have been analysed with the Eiber'model.
A flow stress-values of 36,9 Kg/mm^2 ($\pm$ 24 % s.d.) results, while the U.T.S. of the steel was reported to be 40,7 kg/mm^2. Therefore, in this tubing at high temperature, the Eiber'flow stress would be quite near the U.T.S., while in our results it reached this level in the room temperature tests but was lower in the 540°C tests.
One may therefore conclude that the relation between $\bar{\sigma}$ and the monoaxial tensile properties are geometry dependent and therefore that the Eiber'model may be used for prediction only on the basis of one full scale experiment.
As far as the Carlsson' and Dufresne'models are concerned, C.O.D. tests on specimens conveniently shaped (see above) are in progress in order to check if within some geometry requirements, the C.O.D. entering the model may be evaluated by laboratory tests.

4. Analysis and discussion of the propagation behaviour.

4.1 On fig. 6, the frontiere between full propagation and leakage is fairly well defined : it is about 18-19 kg/mm^2 for 75 mm long cracks and 8-9 Kg/mm^2 for 150 mm long cracks. On the basis of the hypothesis presented in section 1, these stresses should represent the critical stress for instability of the corresponding through cracks.
In a previous work [2][3] based on hydraulic burst test of through cracked tubes, crack instability in tubing identical to that concerned here could be described by a fracture toughness value of 347 kg/mm$^{-3/2}$. The plasticity correction in the derivation of K_c was based on a flow stress value $\bar{\sigma} = \frac{\sigma_y + \sigma_u}{2} = 35$ kg/mm^{-2}. Using these both values and the same analysis, one could calculate the critical stress corresponding to 75 mm and 150 mm long through cracks as :

$$\sigma_h^c = \frac{2}{\pi} \cdot \frac{\bar{\sigma}}{M} \cdot \text{Arc cos} \left[\exp \left(- \frac{\pi}{8a} \cdot \frac{K_c^2}{\bar{\sigma}^2} \right) \right] \qquad \text{eq. (4)}$$

The result plotted on fig. 6 demonstrates a significantly lower instability stress as that evidenced in the part through cracked tubing tests. Indeed this latter is at a level where it is not more dependent of the fracture toughness value, K_c, but reaches the limit value ($K_c \to \infty$ in (4)) :

$$\sigma_h = \frac{\bar{\sigma}}{M} \qquad \text{eq. (5)}$$

while this relationship was definitively unvalid to describe the through cracked tube test results.
The reason for this different behaviour is seen as the result of a dynamic effect : while the hydraulic through cracked (and sealed) tube test is essentially static, the part-through cracked tube test under gas is a dynamic test from the point of view of the loading rate of the through crack created by the ligament rupture and the availability to the through crack of the energy contained in the gas which depends on a balance between the depressurization and the crack propagation rates. It is therefore possible that at the formation of the through crack the nominal gross stress superates the static initiation level but that the crack has no time to propagate before the depressurization of the tube.

4.2. The same analysis cannot be performed directly for the tests at 540°C as no result of through cracked tube tests are available at this temperature. These tests however give an opportunity to check how far a fracture mechanics approach and a specimen test are able to predict the fracture behaviour of the tube at this temperature.
Elasto-plastic fracture mechanics give us the following relationships:

$$\mathcal{G}_c = \frac{K_c^2}{E} = n \bar{\sigma} \delta_c \qquad \text{eq. (6)}$$

in which n is a "constraint factor" which for a plane stress behaviour would be equal to unity. $\bar{\sigma}$ should be equal to σ_y for an elastic-perfect plastic behaviour. One should assume a greater value for a strain-hardening material.
C.O.D. tests on C.T. specimens made in the same steel grade as the tubes [1] indicated the following values for the C.O.D. at initiation for a thickness of 8 mm:

20°C { 700µ (± 3 %) 540°C { 470µ (± 22 %)

Assuming for the tube material the same C.O.D. value, and using relation (6), one can predict : $K_i = \sqrt{E \bar{\sigma} \delta_i}$, which gives, at 20°C, $K_i = 482$ Kg/mm$^{-3/2}$ ($\bar{\sigma} = \sigma_y = 16,6$ kg/mm^2) or $K_i = 863$ Kg/mm$^{-3/2}$ ($\bar{\sigma} = \sigma_u = 53,2$ Kg/mm^2) to be compared to $K_c = 347$ Kg/mm$^{-3/2}$ at instability in the through-cracked tube tests. Therefore a direct or "absolute" prediction of the tube behaviour on the basis of the C.O.D. test would not have been conservative. In this discrepancy the influence of slight differences between the specimen and tube materials could be questioned but it is probable that the validity of relation (6) and that of the analysis on which was based the calculation of K_c in the tube test for a large scale yielding behaviour is certainly a more important factor.

One may however retain from equation (6) that a proportionality relationship should be maintained between K_c^2 and the product $E \bar{\sigma} \delta_c$. On this basis one can write :

$$(K_c)^{540^\circ C}_{tube} = (K_c)^{20^\circ C}_{tube} \times \sqrt{\frac{[E \bar{\sigma} \delta]^{540^\circ C}_{specimen}}{[E \bar{\sigma} \delta]^{20^\circ C}_{specimen}}}$$

Taking $\bar{\sigma} = \frac{\sigma_y + \sigma_u}{2}$ one obtains $(K_c)^{540^\circ}_{tube} \simeq 200$ Kg/mm$^{-3/2}$

The critical stress for crack instability in the tubes at 540°C calculated on the basis of this K_c value is plotted on fig. 7, together with that obtained by $\sigma_c = \bar{\sigma} \cdot M^{-1}$.

Although the part through cracked tube results do not permit to identify with the same precision as at 20°C the instability limit, the prediction by the K_c approach looks again fairly conservative, confirming simultaneously the findings of the room temperature tests and the suitability of the prediction of the results at 540°C based on the C.O.D. tests.

5. Conclusions.

a) Part-through crack failure data relative to thin austenitic s.s. tubes have been analysed by three models relevant to thin and ductile material proposed by Eiber, Carlsson and Dufresne respectively. Although the three models described conveniently the experimental results within the relatively limited range of variation of the crack depth, the Carlsson'model gave slightly better results. The relationship between the flow stress entering the Eiber'model and the tensile properties of the material seems dependent of both geometry and temperature. The capacity of prediction of the two other models on the basis of specimen tests needs to be evaluated on the basis of a representative C.O.D. test presently in progress.

b) The frontiere between leakage and catastrophic failure of the part-through cracked tubes corresponds to a higher toughness than that inferred from through cracked tube tests. This difference is understood as a dynamic loading effect in the part-through cracked tube tests. The prediction of the propagation behaviour based on the results of through cracked tube tests is conservative and suitable for a safety evaluation.

c) A correction to the toughness deduced from through cracked tube test results may be performed to take in account changes in material properties using C.O.D. test data. This procedure was found conservative in the prediction of the propagation behaviour of the part-through cracked tubes burst at high temperature.

Acknowledgements.

The author is indebted to Messrs. Manzotti, Tognoli and Julita for their technical assistance.

REFERENCES

[1] HENRY, B., "Evaluation and significance for LMFBR structures of fracture toughness degradation of austenitic stainless steels due to thermal aging". EUR-report. 1975. To be published.

[2] HENRY B., BERNARD J., "Fracture criteria for type AISI 304 s.s. tubing" in Ispra 1972 annual report. EUR-5060.

[3] BERNARD J., HENRY B., "Etude Experimentale de l'effet de la courbure sur la valeur du facteur d'intensité de contrainte dans les coques cylindriques". EUR-5137.f 1974.

[4] HAHN G.T. et al. Int. Journ. of Fract. Mech. 5, 3 (1969)

[5] EIBER R.J. etal. "Further work on flaw behaviour in pressure vessels". Conf. on Pract. Applic. of Fracture Mech. to Press. vess. Technology. London. May 1971.

[6] CARLSSON A.J., "A fracture model for surface flaws and certain types of weld defects in ductile material". Eng. Fract. Mech. Dec. 1973.

[7] DUFRESNE J., "Failure criteria of part-through cracks in thin walls for elasto-plastic materials sensitive to strain-hardening". To be published in Int. J. of Fract. Mech.

CAPTIONS USED IN THE TEXT

K :	Stress intensity factor (K_c : critical)	$Kg.mm^{-3/2}$
a :	half crack length	mm
R :	tube radius	mm
e :	tube thickness	mm
p :	crack depth	mm
ν :	Poisson'coefficient	-
E :	elasticity modulus	$Kg.mm^{-2}$
σ_y :	yield strength	$Kg.mm^{-2}$
σ_u :	ultimate tensile strength	$Kg.\ mm^{-2}$
M :	magnification factor for curvature	-
δ :	crack opening displacement (δ_c : critical)	mm
δ_C :	δ_c calculated with Carlsson'model	mm
δ_D :	δ_c calculated with Dufresne'model	mm

TABLE I

Reference properties of the tubing

Composition (X Cr Ni 18.11)

C : 0,04 - 0,08	Si ⩽ 0,75	S ⩽ 0,30
Cr : 17,0 - 19,0	Mn ⩽ 2,0	
Ni : 10,0 - 12,0	P ⩽ 0,045	

Results of tensile tests.

a) Flat specimens(1)

°C		$\sigma_{0.2}$ kg/mm²	σ_{R_2} kg/mm²	ε_R %	S %	Remarks
20	L	18.1	53.7	72(2)	53.4	
	T	20.1	53.2	76(2)	56.9	cold flattened specimens
540°	L	13.2	39.1	33(3)	44	
	T	12.6	38.5	33.6(3)	42.4	cold flattened specimens

Notes : (1) each value is the average result of 3 specimens; (2) measured on 5.65 $\sqrt{S}$; (3) measured on 7.3 $\sqrt{S}$.

b) Ring test (ASTM A 370, Supplement 7)
(Monaxial transverse loading)
Ring machined at $\varnothing_i$ 165.3 mm - $\varnothing_e$ 175 mm - thickness : 4.85 mm; height : 75 mm.
Hoop stress at 0.2 % diametral plastic strain = 16.6 kg/mm²
Elasticity modulus along the circumferential direction=19.500 kg/mm²

TABLE III

Results of the burst tests at 540°C

test ref.	2 a (mm)	e (mm)	p (mm)	$p/_c$ -	$\varnothing_c$ (mm)	σ_h^{exp} kg/mm²	$\bar{\sigma}$ kg/mm²	δ_C(1) (mm)	δ_D(2) (mm)	Propagation behaviour
2	75	6,65	4,25	0,6391	177,0	13,64	25,90	0,092	-	P
3	id.	6,35	4,45	0,7008	176,8	12,68	27,96	0,111	-	P
7	id.	5,55	4,16	0,7495	175,5	12,39	32,30	0,137	0,2146	P
8	id.	6,55	5,24	0,8000	177,2	10,02	30,45	0,107	0,0662	I
4	150	6,60	5,10	0,7727	176,4	8,08	27,52	0,073	0,0167	P + A (17,2 cm)
5	id.	5,95	5,05	0,8487	177,0	8,90	44,77	0,222	0,1247	P + A (10,5 cm)
6	id.	6,20	5,27	0,8500	176,9	6,80	34,32	0,118	0,0477	P + A (4,4 cm)
							29,6 (3)	0,107 (4)	0,094	mean
							± 3,5 (12%)	±0,02 (20%)	±0,078 (83%)	standard deviation

(1) calculated with $\bar{\sigma} = \frac{\sigma_y + \sigma_u}{2}$ = 25,5 kg/mm2 and E=13.375 kg/mm²
(2) calculated with σ_y = 12,6 , σ_u = 38,5 , E=13.375 kg/mm² xx see page9

TABLE II

Results of the burst tests at 20°C

test ref.	2 a (mm)	e (mm)	p (mm)	p/e -	ϕ_e (mm)	q_h^{exp} (kg/mm^2)	$\bar{\sigma}$ kg/mm^2	δ_c (1) (mm)	δ_D (2)	Propagation behaviour	Notes
4	75	5,70	4,00	0,7018	176,3	21,55	48,56	0,19	-	P	
11	id.	6,00	4,60	0,7667	176,6	19,00	51,70	0,17	-	P	
5	id.	5,85	4,64	0,7932	176,1	18,12	54,83	0,17	-	I	
7	id.	5,90	4,70	0,7966	176,2	18,81	57,57	0,19	-	I	
12	id.	5,96	5,13	0,8607	176,8	15,73	66,66	0,17	0,181	L	
6	150	5,70	4,45	0,7807	175,85	15,19	54,37	0,22	0,204	P	
1	id.	4,79	4,02	0,8392	175,7	12,82	62,54	0,21	0,133	(L)	Pressurized with water
9	id.	6,20	5,27	0,8500	177,0	11,33	57,19	0,18	0,101	P	
8	id.	5,82	5,20	0,8935	176,1	10,24	72,46	0,19	0,102	P+A(0,7cm)	
3	id.	5,52	4,96	0,8986	176,5	8,66	64,46	0,14	0,070	I	
2	id.	5,75	5,17	0,8991	176,7	9,67	71,99	0,18	0,093	(L)	Pressurized with water
10	id.	5,96	5,54	0,9295	176,5	6,49	68,05	0,11	0,052	L	
							60,87	0,17	0,117		mean
							± 7,96	±0,03	±0,053		stand.dev.
							(13%)	(17,6%)	(45%)		

(1) Calculated with $\bar{\sigma} = \frac{\sigma_y + \sigma_u}{2} = 35$ kg.mm^{-2} and E = 20.300 kg/mm^2

(2) Calculated with $\sigma_y = 16,6$, $\sigma_u = 53,2$ kg/mm^2 , E = 20.300 kg/mm^2

xx (TABLE III)

(3) Without taking in account test nr. 5

(4) id. with test nr. 5, $\bar{\delta}_c = 0,123$ mm

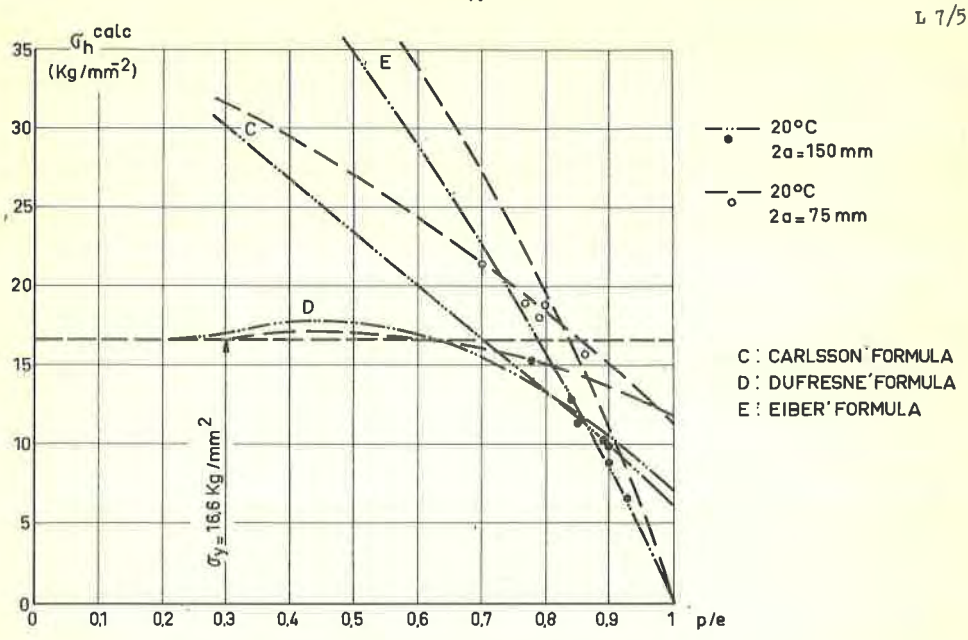

Fig. 1 Gross Hoop Stress at Failure Vs. Ratio Crack Depth/Wall thickness (20° C)

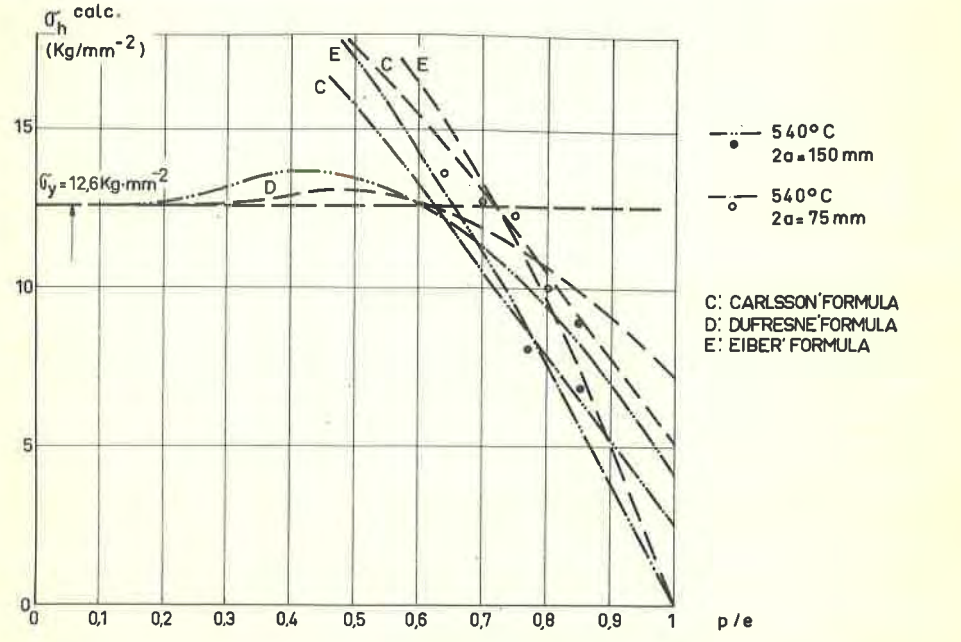

Fig. 2 Gross Hoop Stress at Failure Vs. Ratio Crack Depth/Wall thickness (540°C)

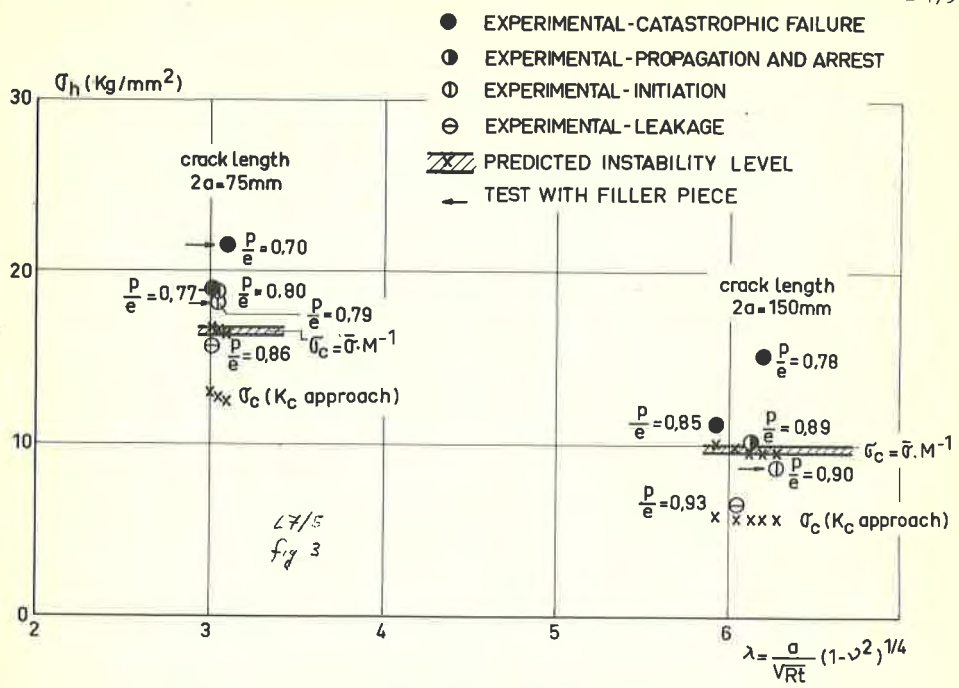

Fig. 3 Gross Hoop Stress at Failure Vs. the Shell Parameter λ and Propagation Behaviour. (Tests at 20° C).

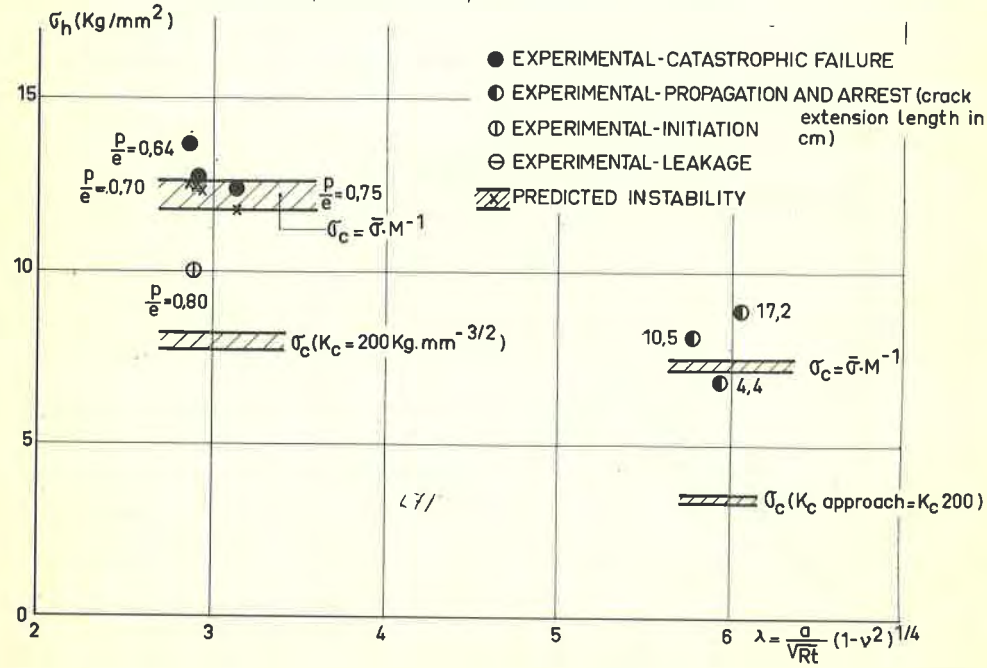

Fig. 4 Gross Hoop Stress at Failure Vs. the Shell Parameter λ and Propagation Behaviour. (Tests at 40° C).

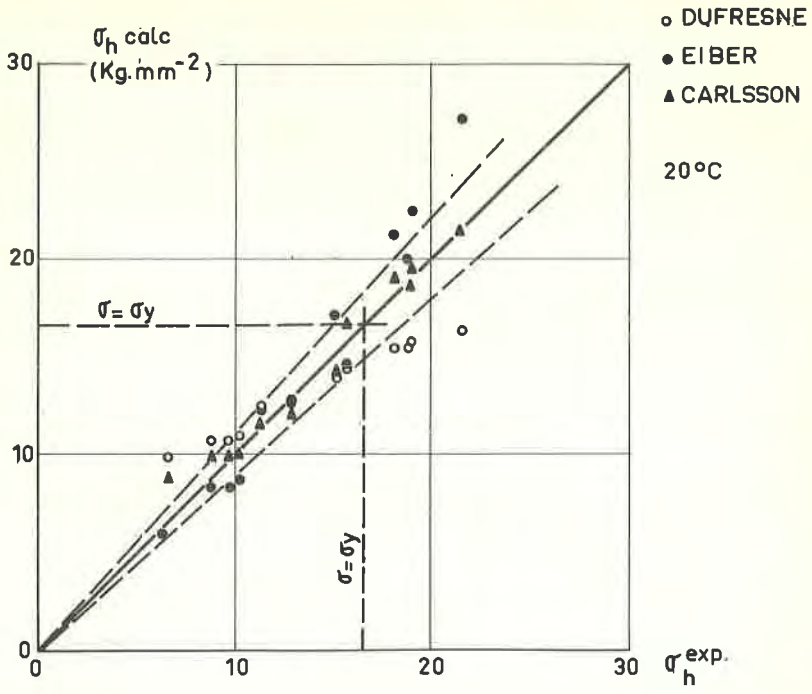

Fig. 5 Comparison of calculated and experimental Gross Hoop Stress at Ligament Failure. (Tests at 20° C).

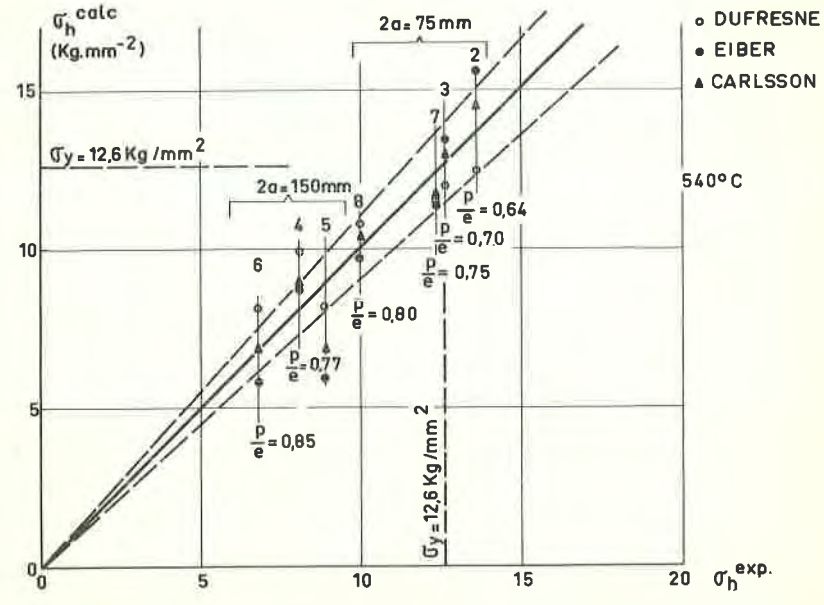

Fig. 6 Comparison of calculated and Experimental Gross Hoop Stress at Ligament Failure (Tests at 540° C).